

Experimental Determination of Phase Equilibria in the Sn-Zn-Sb System

Cuiping Wang, Yelu Xu, Shuiyuan Yang, Hengxing Jiang, Jian Li, Jiahua Zhu, Shuang Yang, and Xingjun Liu

(Submitted September 9, 2014; in revised form April 8, 2015; published online July 2, 2015)

The phase equilibria of the Sn-Zn-Sb ternary system at 400 and 500 °C were experimentally determined by electron probe microanalyzer, x-ray diffraction and differential scanning calorimetry. In this study, the ternary compound of (Zn,Sn)Sb is confirmed at 400 and 500 °C. Additionally, a liquid phase region is found at 400 °C with composition ranges of 9.09–12.86 at.% Zn and 31.47–34.22 at.% Sn, which becomes a prolongation of the main liquid as the temperature is raised to 500 °C.

Keywords microstructure, phase diagrams, ternary alloy systems

1. Introduction

Concerns over the toxicity of lead have resulted in motivation to eliminate the use of solders containing Pb, and to multifarious efforts to replace lead-containing solder.^[1] Since Sn-Zn based alloys have low melting temperature, good properties and are inexpensive, they have been considered as a good candidate to replace Sn-Pb eutectic alloys.^[2–4] Also Sb and Zn are common components in alloys developed for lead-free soldering.^[5,6] Thus Sn-Zn-Sb ternary alloys may be potential lead-free solders, and knowledge of its phase equilibrium will be necessary for the development of Sn-Zn-Sb ternary alloys.

In the previous experimental work, Zobac et al.^[7] obtained information on the thermodynamic stability of the coexisting phase by using DTA method at 200, 250 and 350 °C.^[7] However the phase equilibrium and the microstructure of the Sn-Zn-Sb ternary system at higher temperature are lacking. Positioning of the phase fields with mutual solubility of all three components and specification of the stability range of the ternary phase depend on the experimental research of the Sn-Zn-Sb ternary system.^[7]

In the present work, the phase equilibrium of the Sn-Zn-Sb system at 400 and 500 °C were experimentally determined by using electron probe microanalyzer (EPMA), x-ray diffraction (XRD) and differential scanning calorime-

try (DSC). The obtained results are expected to give a better understanding on microstructures in the Sn-Zn-Sb alloys.

Three binary systems Sb-Zn,^[8] Sb-Sn^[9] and Sn-Zn,^[10] constituting the Sn-Zn-Sb ternary system, are shown in Fig. 1. The Sb-Zn binary system has been studied by many researchers.^[11–15] The Sb-Zn binary phase diagram assessed by Li et al.^[8] is adopted in this work due to the good agreement with the experimental data. The Sb-Zn binary system has six intermediate phases, namely SbZn, γ -Sb₃Zn₄, β -Sb₃Zn₄, α -Sb₃Zn₄, β -Sb₂Zn₃ and α -Sb₂Zn₃, respectively. The phase diagram of the Sn-Zn binary system is a simple system without any intermediate phase. The Sb-Sn^[9,16–19] binary system has two intermediate phases, Sb₂Sn₃ and SbSn phases. There are three peritectic reactions, $L + Sb_2Sn_3 \leftrightarrow Sn$, $L + SbSn \leftrightarrow Sb_2Sn_3$, and $L + Sb \leftrightarrow SbSn$ in the Sb-Sn binary system, occurring at 243, 323 and 424 °C, respectively. The information of all stable solid phases in the three binary and ternary systems mentioned above is summarized in Table 1. It is notable that Sb₂SnZn phase can exist as a polymorph as reported by Tenga et al.^[21]: chalcocopyrite phase (space group: *I*-42*d*) below 240 °C, and sphalerite phase (space group: *F*-43*m*) above 240 °C.

2. Experimental Procedures

Sn-Zn-Sb alloys were prepared using pure antimony (99.8 wt.%), zinc (99.8 wt.%) and tin (99.9 wt.%) in sealed transparent quartz capsules. In order to reduce the volatilization of zinc and ensure the samples homogeneity, the capsules were placed in argon atmosphere at 300 °C for 24 h. After that, the alloys were annealed at 800 °C for 72 h.

Afterwards, the samples were cut into small pieces. All samples were sealed in quartz capsules that are evacuated and backfilled with argon gas. The samples were annealed at 400 and 500 °C, respectively. On the basis of the temperature and composition of the samples, time of the heat treatment varied from several hours to several days. At the end of the heat treatment, the samples were quenched into ice water.

Cuiping Wang, Shuiyuan Yang, Hengxing Jiang, Jian Li, Jiahua Zhu, Shuang Yang, and Xingjun Liu, Department of Materials Science and Engineering, College of Materials, Xiamen University, Xiamen 361005, People's Republic of China and Research Center of Materials Design and Applications, Xiamen University, Xiamen 361005, People's Republic of China; and Yelu Xu, Department of Materials Science and Engineering, College of Materials, Xiamen University, Xiamen 361005, People's Republic of China. Contact e-mail: lxj@xmu.edu.cn.

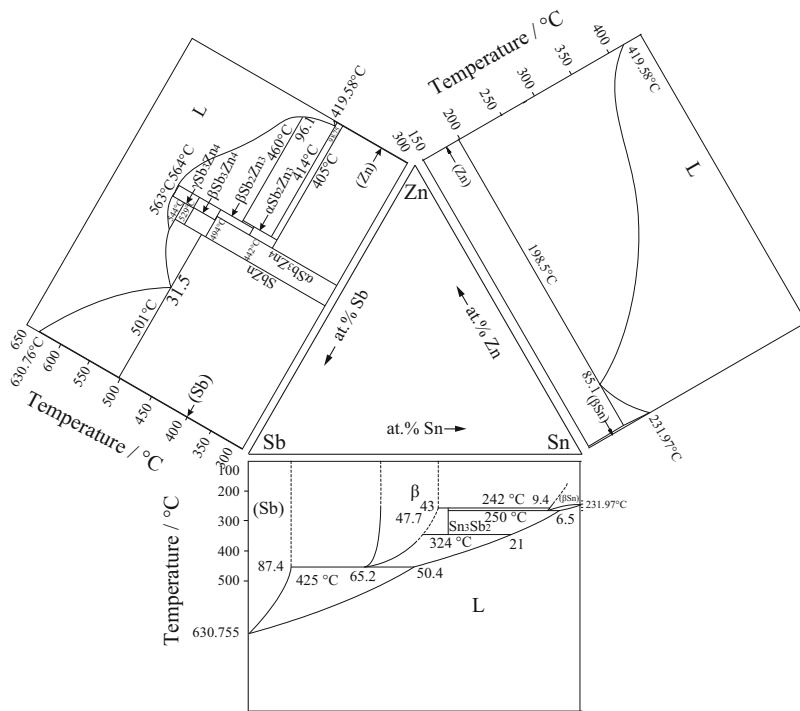


Fig. 1 Binary phase diagrams constituting the Sn-Zn-Sb ternary system^[8]

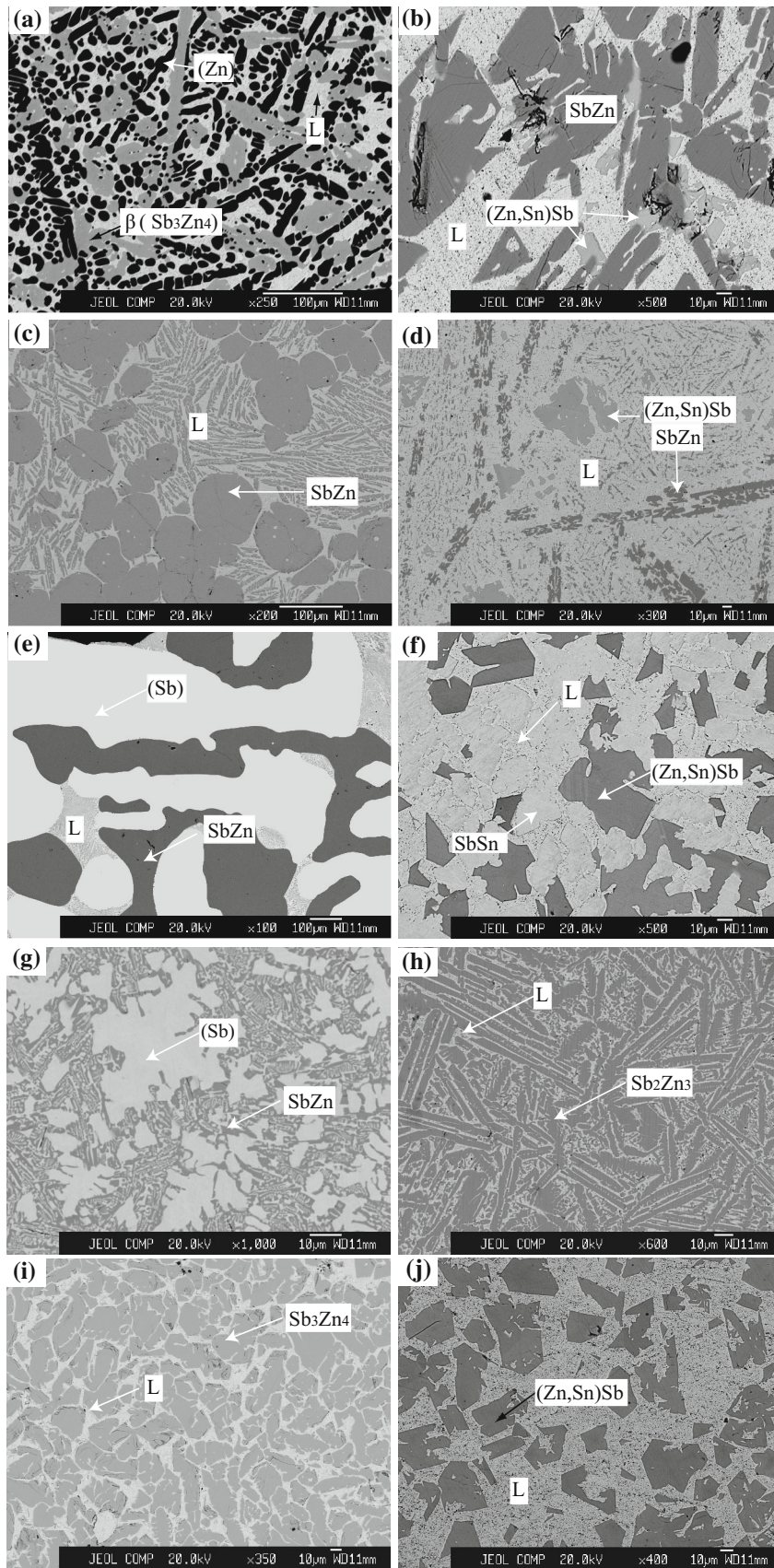
Table 1 The stable solid phases in three binary systems

System	Phase	Pearson's symbol	Prototype	Space group	Strukturbericht	References
Sb-Zn	(Sb)	<i>hR2</i>	α As	<i>R-3 m</i>	<i>A7</i>	[8]
	SbZn	<i>oP16</i>	CdSb	<i>Pbca</i>	<i>Be</i>	[8]
	γ Sb ₃ Zn ₄	[8]
	β Sb ₃ Zn ₄	[8]
	α Sb ₃ Zn ₄	<i>oP28</i>	...	<i>Pmmn</i>	...	[8]
	β Sb ₂ Zn ₃	<i>oI*</i>	[8]
	α Sb ₂ Zn ₃	<i>oP32</i>	...	<i>Pmmn</i>	...	[8]
Sb-Sn	(Zn)	<i>hP2</i>	Mg	<i>P6₃/mmc</i>	<i>A3</i>	[8]
	(βSn)	<i>tI4</i>	BSn	<i>I4₁/amd</i>	<i>A5</i>	[9]
	Sn ₃ Sb ₂	[9]
Zn-Sn	βSbSn	<i>cF8</i>	NaCl	<i>Fm-3 m</i>	<i>B1</i>	[9]
	(Sb)	<i>hR2</i>	α As	<i>R-3 m</i>	<i>A7</i>	[9]
	(Zn)	<i>hP2</i>	Mg	<i>P6₃/mmc</i>	<i>A3</i>	[10]
Sn-Zn-Sb	(βSn)	<i>tI4</i>	BSn	<i>I4₁/amd</i>	<i>A5</i>	[10]
	(Zn,Sn)Sb	...	ZnS(sphalerite)	<i>F-43 m(h)</i>	...	[7, 21]
	Sb ₂ SnZn	...	CuFeS ₂	<i>I-42d(l)</i>	...	[7, 21]

h high temperature, *l* low temperature

Compositions of the phases were determined using EPMA (JXA-8100R, JEOL, Japan). Pure elements were used as standards and the measurements were carried out at a voltage of 20 kV and a current of 20 nA. Microprobe measurements for each equilibrium phase were taken on seven points to get high accuracy. The composition of the liquid phase was determined via area analysis using EDS at 20.0 kV. Seven area measurements on the liquid phase were

made to decrease the statistical error. At the same time, the maximum and minimum values were removed, and the final values were the average of the remaining values. The constituent phases of the alloys were further determined by analyzing XRD patterns generated by a Phillips PANalytical X-pert diffractometer, operating at 40.0 kV and 30 mA with Cu K α radiation. The data were collected in the range of 2 θ from 20° to 90° at a step size of 0.0167°. The phase



◀ **Fig. 2** Typical ternary BSE images obtained from: (a) $\text{Sn}_{20}\text{Zn}_{70}\text{Sb}_{10}$ (at.%) alloy annealed at 400 °C for 4 days; (b) $\text{Sn}_{35}\text{Zn}_{32}\text{Sb}_{33}$ (at.%) alloy annealed at 400 °C for 18 days; (c) $\text{Sn}_{20}\text{Zn}_{40}\text{Sb}_{40}$ (at.%) alloy annealed at 400 °C for 4 days; (d) $\text{Sn}_{26}\text{Zn}_{23}\text{Sb}_{51}$ (at.%) alloy annealed at 400 °C for 4 days; (e) $\text{Sn}_{10}\text{Zn}_{20}\text{Sb}_{70}$ (at.%) alloy annealed at 400 °C for 18 days; (f) $\text{Sn}_{50}\text{Zn}_{10}\text{Sb}_{40}$ (at.%) alloy annealed at 400 °C for 4 days; (g) $\text{Sn}_3\text{Zn}_{20}\text{Sb}_{77}$ (at.%) alloy annealed at 500 °C for 30 days; (h) $\text{Sn}_{20}\text{Zn}_{50}\text{Sb}_{30}$ (at.%) alloy annealed at 500 °C for 2 days; (i) $\text{Sn}_{20}\text{Zn}_{45}\text{Sb}_{35}$ (at.%) alloy annealed at 500 °C for 2 days; (j) $\text{Sn}_{65}\text{Zn}_{10}\text{Sb}_{25}$ (at.%) alloy annealed at 500 °C for 2 days

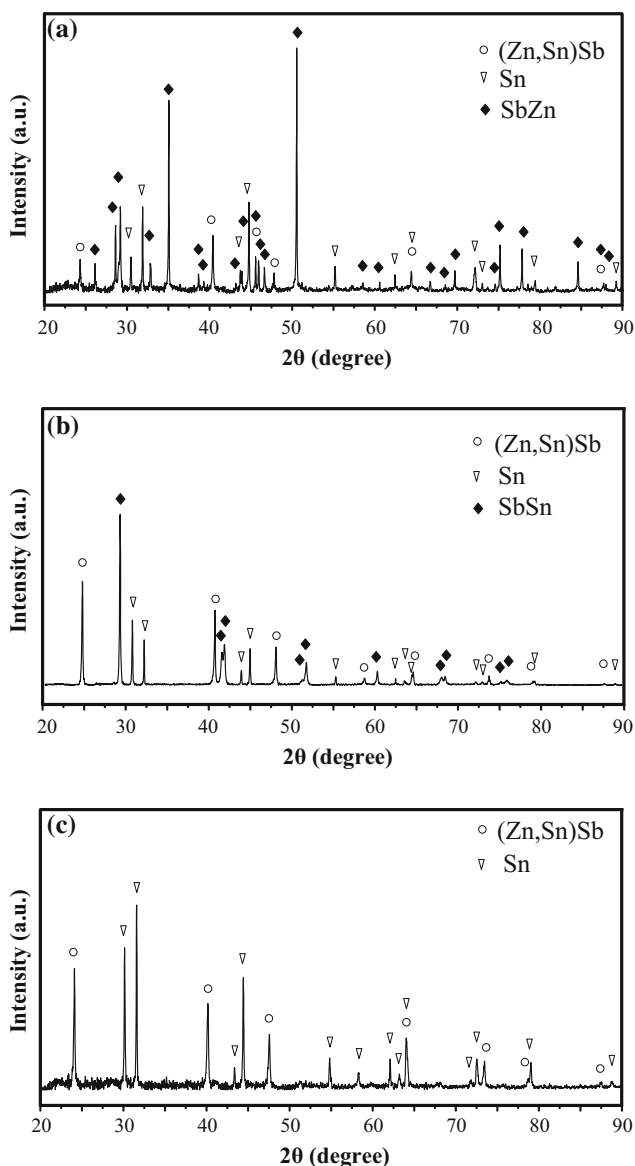


Fig. 3 X-ray diffraction patterns obtained from: (a) $\text{Sn}_{35}\text{Zn}_{32}\text{Sb}_{33}$ (at.%) alloy annealed at 400 °C for 18 days; (b) $\text{Sn}_{50}\text{Zn}_{10}\text{Sb}_{40}$ (at.%) alloy annealed at 400 °C for 4 days; (c) $\text{Sn}_{65}\text{Zn}_{10}\text{Sb}_{25}$ (at.%) alloy annealed at 500 °C for 2 days

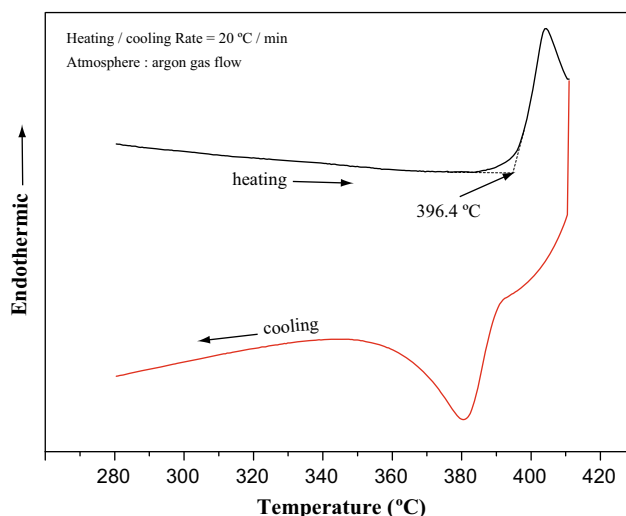


Fig. 4 DSC heating and cooling curves of the $\text{Sn}_{10}\text{Zn}_{20}\text{Sb}_{70}$ (at.%) alloy

transformation temperature was determined using DSC (DSC-404C, NETZSCH, Germany) test. And the measurements were conducted using small pieces of specimens ranging from 18 to 44 mg at a heating and cooling rates of 20 °C/min in a flowing argon atmosphere with sintered Al_2O_3 as reference.

3. Results and Discussion

3.1 Microstructure and Phase Equilibria

Back-scattered electron (BSE) images of typical ternary Sn-Zn-Sb alloys are shown Fig. 2(a)-(j). Phase identification is based on the equilibrium composition measured by EPMA and crystal structure determined by XRD analysis. For the $\text{Sn}_{20}\text{Zn}_{70}\text{Sb}_{10}$ (at.%) alloy quenched from 400 °C, three phases microstructure is observed, as showed in Fig. 2(a). EPMA result indicates that the dark phase is (Zn), the grey one is $\beta(\text{Sb}_3\text{Zn}_4)$, and the white one is Liquid (denoted as “L” in this study). This liquid phase is located in the Sn-rich region. Another liquid phase region is found in the Sb-rich region at 400 °C and will be discussed later in the following. Figure 2(b) shows three phases microstructure of the $\text{SbZn} + (\text{Zn,Sn})\text{Sb} + \text{L}$ in the $\text{Sn}_{35}\text{Zn}_{32}\text{Sb}_{33}$ (at.%) alloy. These results have been confirmed by XRD analysis. XRD patterns of the $\text{Sn}_{35}\text{Zn}_{32}\text{Sb}_{33}$ (at.%) alloy show characteristic peaks of Sn phase. So the existence of a liquid phase is confirmed. In the quenching process, it is inevitable the liquid phase decomposing to several solid phase, probably into Sn and either SbSn or Zn phase. After analyzing XRD result, we find that the characteristic peaks corresponding to SbSn or Zn phase are covered by those of SbZn phase. Although the liquid decomposes into either SbSn or Zn phase is reasonable from the binary phase diagrams, we haven't found clear evidence to confirm the

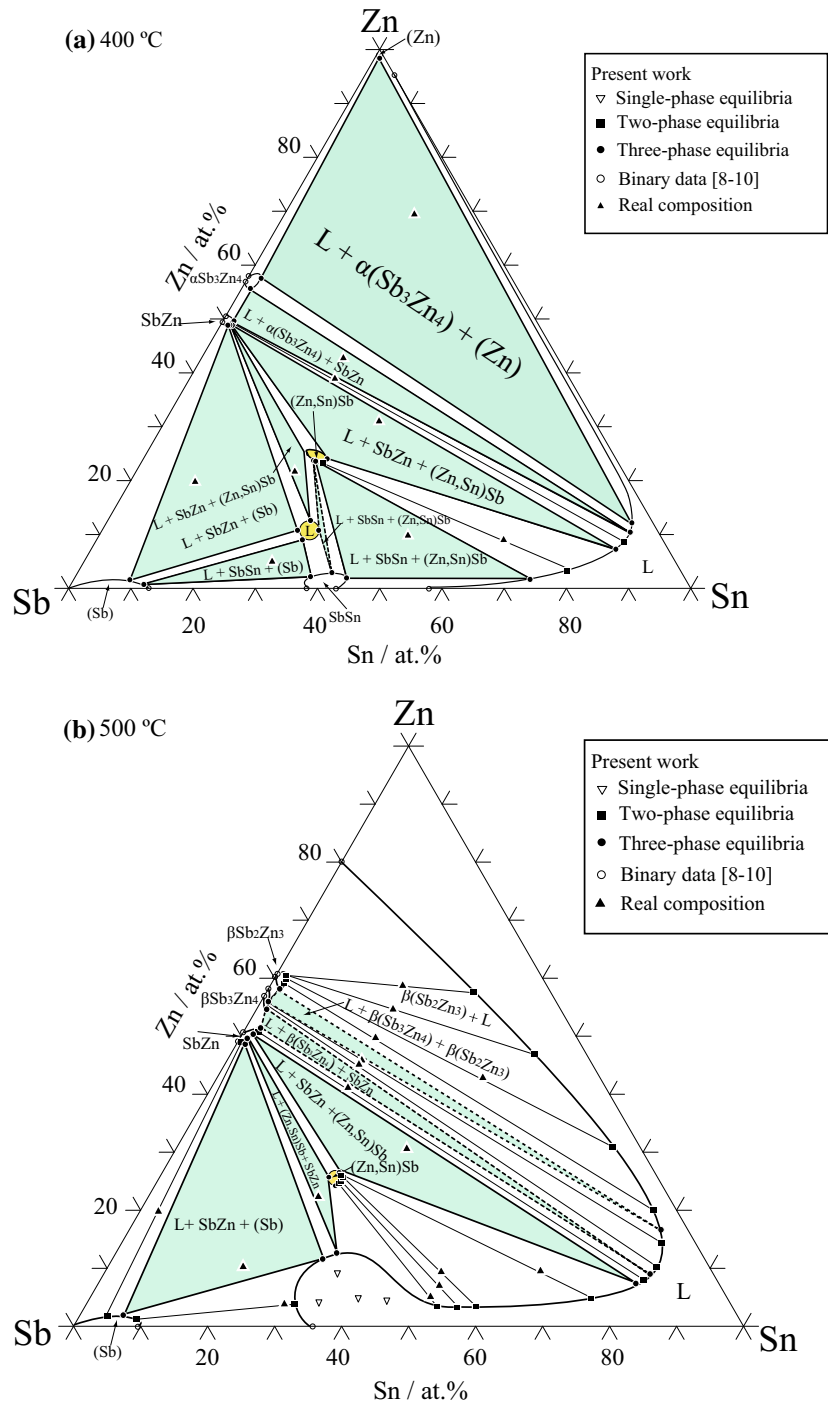


Fig. 5 Experimentally determined isothermal sections of the Sn-Zn-Sb system at (a) 400 °C and (b) 500 °C

existence of SbSn or Zn phase. As shown in Fig. 3(a), it can be seen the characteristic peaks corresponding to Sn, SbZn and (Zn,Sn)Sb phases are well distinguished by different symbols. The BSE micrograph of the Sn₂₀Zn₄₀Sb₄₀ (at.%) alloy annealed at 400 °C for 4 days is showed in Fig. 2(c), where two different phases (SbZn + L) are distinguished. Three-phase microstructure of the L + (Zn,Sn)Sb + SbZn in

the Sn₂₆Zn₂₃Sb₅₁(at.%) alloy annealed at 400 °C for 4 days is shown in Fig. 2(d). BSE image of the Sn₁₀Zn₂₀Sb₇₀ (at.%) alloy annealed at 400 °C for 18 days is presented in Fig. 2(e), showing coexistence of three phases consisted of SbZn + (Sb) + L. To confirm the existence of the liquid phase, a DSC test for Sn₁₀Zn₂₀Sb₇₀ (at.%) alloy was then carried out. As shown in Fig. 4, it can be seen that there is

Table 2 Equilibrium compositions of the Sb-Zn-Sn ternary system determined in the present work

Temperature, °C	Nominal composition, at.%	Real composition, at.%	Annealed time, days or h	Phase equilibria	Composition, at.%					
					Phase 1		Phase 2		Phase 3	
					Zn	Sn	Zn	Sn	Zn	Sn
400	Sn ₂₀ Zn ₇₀ Sb ₁₀	Sn _{21.17} Zn _{69.57} Sb _{9.26}	4 days	Liquid/ α (Sb ₃ Zn ₄)/(Zn)	12.42	84.92	58.31	1.69	98.23	0.70
	Sn ₂₀ Zn ₄₅ Sb ₃₅	Sn _{22.82} Zn _{43.18} Sb ₃₄	4 days	Liquid/ α (Sb ₃ Zn ₄)/SbZn	9.98	85.57	55.43	1.60	49.45	1.53
	Sn ₂₀ Zn ₄₀ Sb ₄₀	Sn _{23.39} Zn _{38.97} Sb _{37.64}	4 days	Liquid/SbZn	8.65	84.70	49.22	1.64
	Sn ₁₀ Zn ₂₀ Sb ₇₀	Sn _{11.17} Zn _{19.04} Sb _{68.79}	18 days	Liquid/SbZn/Sb	10.86	31.47	48.78	1.29	1.33	9.14
	Sn ₂₆ Zn ₂₃ Sb ₅₁	Sn _{25.23} Zn _{21.1} Sb _{53.67}	4 days	Liquid/SbZn/(Zn,Sn)Sb	12.86	32.39	48.78	1.67	25.28	25.39
	Sn ₃₅ Zn ₃₂ Sb ₃₃	Sn _{34.56} Zn _{30.89} Sb _{34.55}	18 days	Liquid/SbZn/(Zn,Sn)Sb	7.32	84.21	48.78	1.86	23.73	29.82
	Sn ₃₀ Zn ₅ Sb ₆₅	Sn _{30.44} Zn _{4.89} Sb _{64.67}	4 days	Liquid/SbSn/Sb	9.31	33.02	2.22	37.93	0.89	12.05
	Sn ₅₀ Zn ₁₀ Sb ₄₀	Sn _{49.72} Zn _{9.78} Sb _{40.5}	4 days	Liquid/(Zn,Sn)Sb/SbSn	1.77	73.53	23.73	27.90	1.77	43.92
500	Sn ₆₅ Zn ₁₀ Sb ₂₅	Sn _{65.67} Zn _{8.67} Sb _{25.66}	4 days	Liquid/(Zn,Sn)Sb	3.55	78.60	23.50	28.97
	Sn ₂₀ Zn ₆₀ Sb ₂₀	Sn _{19.68} Zn _{58.58} Sb _{21.74}	2 days	Liquid/ β (Sb ₂ Zn ₃)	57.43	31.12	60.53	1.92
	Sn ₂₀ Zn ₅₅ Sb ₂₅	Sn _{20.47} Zn _{54.44} Sb _{25.09}	2 days	Liquid/ β (Sb ₂ Zn ₃)	47.01	44.78	60.31	1.84
	Sn ₄₀ Zn ₄₅ Sb ₁₅	Sn _{39.72} Zn _{42.6} Sb _{17.68}	2 days	Liquid/ β (Sb ₂ Zn ₃)	30.82	65.37	59.87	2.06
	Sn ₂₀ Zn ₅₀ Sb ₃₀	Sn _{20.16} Zn _{49.41} Sb _{30.43}	2 days	Liquid/ β (Sb ₂ Zn ₃)	19.73	77.06	59.20	2.01
	Sn ₂₀ Zn ₄₇ Sb ₃₃	Sn _{19.89} Zn _{45.86} Sb _{34.25}	2 days	Liquid/ β (Sb ₃ Zn ₄)	14.19	80.80	55.43	1.21
	Sn ₂₀ Zn ₄₅ Sb ₃₅	Sn _{19.97} Zn _{44.67} Sb _{35.36}	2 days	Liquid/ β (Sb ₃ Zn ₄)	10.20	81.84	54.99	1.44
	Sn ₂₀ Zn ₄₀ Sb ₄₀	Sn _{20.35} Zn _{39.04} Sb _{40.61}	2 days	Liquid/SbZn	8.20	80.54	50.78	2.01
	Sn ₂₀ Zn ₁₀ Sb ₇₀	Sn _{19.84} Zn _{9.76} Sb _{70.4}	18 days	Liquid/SbZn/(Sb)	11.75	31.54	48.56	1.20	1.77	6.60
	Sn ₃ Zn ₂₀ Sb ₇₇	Sn _{2.8} Zn _{19.53} Sb _{77.67}	30 days	SbZn/(Sb)	48.78	0.51	1.77	4.10
500	Sn ₃₀ Zn ₅ Sb ₆₅	Sn _{29.51} Zn _{3.55} Sb _{66.94}	2 days	Liquid/(Sb)	4.88	37.37	1.33	8.57
	Sn ₃₅ Zn ₅ Sb ₆₀	Sn _{34.73} Zn _{3.91} Sb _{61.36}	2 h	Liquid	3.91	34.73
	Sn ₅₀ Zn ₁₀ Sb ₄₀	Sn _{50.28} Zn _{9.17} Sb _{40.55}	2 days	Liquid/(Zn,Sn)Sb	3.82	58.12	25.06	27.56
	Sn ₆₅ Zn ₁₀ Sb ₂₅	Sn _{65.16} Zn _{9.17} Sb _{25.67}	2 days	Liquid/(Zn,Sn)Sb	4.70	75.23	25.72	27.81
	Sn ₃₅ Zn ₃₂ Sb ₃₃	Sn _{34.51} Zn _{30.47} Sb _{35.02}	2 days	Liquid/(Zn,Sn)Sb/SbZn	7.54	80.01	26.83	26.29	50.33	1.46
	Sn ₂₆ Zn ₂₃ Sb ₅₁	Sn _{25.31} Zn _{22.19} Sb _{52.5}	2 days	Liquid/(Zn,Sn)Sb/SbZn	13.08	32.60	25.72	25.12	49.67	1.22
	Sn ₅₂ Zn ₇ Sb ₄₁	Sn _{51.21} Zn _{6.8} Sb _{41.99}	2 days	Liquid/(Zn,Sn)Sb	3.14	55.95	25.28	27.17
	Sn ₅ Zn ₄ Sb ₄₅	Sn _{51.11} Zn _{3.87} Sb _{45.02}	2 days	Liquid/(Zn,Sn)Sb	3.27	53.04	24.44	27.53
	Sn ₄₅ Zn ₅ Sb ₅₀	Sn _{44.02} Zn _{4.89} Sb _{51.09}	2 h	Liquid	4.89	44.02
	Sn ₃₅ Zn ₁₀ Sb ₅₅	Sn _{34.93} Zn _{9.87} Sb _{55.2}	2 h	Liquid	9.87	34.93
	Sn ₄₀ Zn ₅ Sb ₅₅	Sn _{39.83} Zn _{4.63} Sb _{55.54}	2 h	Liquid	4.63	39.83

Seven analyses were carried out for each phase and the standard deviation of the measured concentration is ± 0.5 at.%

only one melting peak in the heating curve, in which the onset temperature is 396.4 °C. Clearly, the liquid phase appearing at 400 °C for this alloy is proved reasonable since the temperature applied in the phase equilibrium experiments is slightly higher than that in the DSC test. Figure 2(f) shows three-phase equilibrium microstructure consisted of the L + (Zn,Sn)Sb + SbSn for the Sn₅₀Zn₁₀Sb₄₀ (at.%) alloy annealed at 400 °C. This observation is consistent with the analysis of XRD in Fig. 3(b). In Fig. 3(b), the diffraction peaks of the Sn phase, (Zn,Sn)Sb phase and SbSn phase are well identified and marked by different symbols.

In addition, the microstructure of Sn₃Zn₂₀Sb₇₇ (at.%) alloy annealed at 500 °C for 30 days is shown in Fig. 2(g), where there exists a two-phase equilibrium ((Sb) + SbZn). In the Sn₂₀Zn₅₀Sb₃₀ (at.%) alloy quenched from 500 °C, the two-phase microstructure (Sb₂Zn₃ + L) is observed

(Fig. 2h). Figure 2(i) shows the two-phase microstructure (Sb₃Zn₄ + L) of the Sn₂₀Zn₄₅Sb₃₅ (at.%) alloy annealed at 500 °C for 2 days. In the Sn₆₅Zn₁₀Sb₂₅ (at.%) alloy quenched from 500 °C, a two-phase microstructure of the L + (Zn,Sn)Sb is observed in Fig. 2(j). The XRD pattern of this sample is presented in Fig. 3(c), confirming the coexistence of two phases consisted of L + (Zn,Sn)Sb.

3.2 Isothermal Sections

All phase equilibria and related equilibrium compositions of the Sn-Zn-Sb ternary system at 400 and 500 °C determined in the present work by EPMA are summarized in Table 2. Based on the experimental data mentioned above, two isothermal sections at 40 and 500 °C have been constructed as presented in Fig. 5(a) and (b), respectively. Undetermined three-phase regions have dashed outlines.

In the isothermal section at 400 °C shown in Fig. 5(a), eight three-phase regions, two liquid regions and one ternary phase are experimentally determined. The solubility of Sn and Sb in (Zn) is extremely low, and the solubility of Sn in the α (Sb₃Zn₄) and SbZn phase is about 1.69 and 1.29 at.% through the determined isothermal section. In addition, the solubility of Zn in the (Sb) is measured to be approximately 1.33 at.%, and the solubility of Zn in the SbSn phase is measured to be about 2.22 at.%. It is interesting that a region of liquid phase appears at 400 °C in the composition ranges of 9.09-12.86 at.% Zn and 31.47-34.22 at.% Sn, which becomes a prolongation of the main liquid field when the temperature is raised up to 500 °C.

In the isothermal section at 500 °C (Fig. 5b), three three-phase regions of the L + (Zn,Sn)Sb + SbZn, L + (Sb) + SbZn and L + (Zn,Sn)Sb + SbZn are experimentally determined in this work. Compared with the isothermal section at 400 °C, the phase region of the ternary phase (Zn,Sn)Sb phase does not seem to be significantly different. In the previous study, Rinco et al.^[20] considered the (Zn,Sn)Sb could only be stable below 759 K (486 °C). In addition, Tenga et al.^[21] thought that (Zn,Sn)Sb intermetallic phase decomposes peritectically at about 360 °C, and cannot exist stably at 400 and 500 °C. This experimental result is different from the previous literature, because the (Zn,Sn)Sb phase can exist stably as an equilibrium phase at 400 and 500 °C, as measured by EPMA and substantiated by the XRD results, respectively.

4. Conclusions

Two isothermal sections of the Sn-Zn-Sb ternary system at 400 and 500 °C were experimentally determined. The newly determined phase equilibria will provide additional support for the thermodynamic assessment of this Sn-Zn-Sb system. The conclusions drawn from the present study are as follows:

- (1) A liquid phase region is found at 400 °C with composition ranges of 9.09-12.86 at.% Zn and 31.47-34.22 at.% Sn, and the area of liquid phase becomes a prolongation of the main liquid field when the temperature is raised to 500 °C.
- (2) The ternary compound of (Zn,Sn)Sb is confirmed to exist stably at 400 and 500 °C.

Acknowledgments

This work was supported by the National Natural Science Foundation of China (Nos. 51031003 and 51171159) and the Ministry of Education of China (Grant No. 20120121130004). The support from National Key Basic Research Program of China (973 Program, 2012CB825700), the Aviation Industry Corporation of

China and Xiamen City Department of Science & Technology (Grant No. 3502Z20121153) are also acknowledged.

References

1. M.E. Loomans, S. Vaynman, G. Ghosh, and M.E. Fine, Investigation of Multi-component Lead-Free Solders, *J. Electron. Mater.*, 1994, **23**, p 741-746
2. M. Abtey and G. Selvaduray, Lead-Free Solders in Microelectronics, *Mater. Sci. Eng. R*, 2000, **27**, p 95-141
3. C.W. Huang and K.L. Lin, Interfacial Reactions of Lead-Free Sn-Zn Based Solders on Cu and Cu Plated Electroless Ni-P/Au Layer Under Aging at 150 °C, *J. Mater. Res.*, 2004, **19**, p 3560-3568
4. S.W. Chen, C.H. Wang, S.K. Lin, and C.N. Chiu, Phase Diagrams of Pb-free Solders and Their Related Materials Systems, *J. Mater. Sci.*, 2007, **18**, p 19-37
5. T.C. Chang, M.C. Wang, and M.H. Hon, Thermal Properties and Interfacial Reaction Between the Sn-9Zn-xAg Lead-Free Solders and Cu Substrate, *Metall. Mater. Trans. A*, 2005, **36**, p 3019-3029
6. D.R. Frear and P.T. Vianco, Intermetallic Growth and Mechanical Behavior of Low and High Melting Temperature Solder Alloys, *Metall. Mater. Trans. A*, 1994, **25**, p 1509-1523
7. O. Zobac, J. Sopousek, J. Bursik, A. Zemanova, and P. Roupcova, Experimental Study of the Sb-Sn-Zn Alloy System, *Metall. Mater. Trans. A*, 2014, **45**, p 1181-1188
8. J.B. Li, M.C. Record, and J.C. Tedenac, A Thermodynamic Assessment of the Sb-Zn System, *J. Alloy. Compd.*, 2007, **438**, p 171-177
9. B. Predel and W. Schwermann, Constitution and Thermodynamics of Antimony-Tin System, *J. Inst. Met.*, 1971, **99**, p 169-173
10. Z. Moser, J. Dutkiewicz, W. Gasior, and J. Salawa, The Sn-Zn (Tin-Zinc) System, *J. Phase Equilib.*, 1985, **6**, p 330-334
11. G. Vuillard and J.P. Piton, Transformations of Intermetallic Phases of the Antimony-Zinc Systems, *Comput. Rend. Acad. Sci.*, 1966, **263**, p 1018-1021
12. X.J. Liu, C.P. Wang, I. Ohnuma, R. Kainuma, and K. Ishida, Thermodynamic Assessment of the Phase Diagrams of the Cu-Sb and Sb-Zn Systems, *J. Phase Equilib.*, 2000, **21**, p 432-442
13. V. Izard, M.C. Record, J.C. Tedenac, and S.G. Fries, Discussion on the Stability of the Antimony Zinc Binary Phases, *CALPHAD*, 2001, **25**, p 567-581
14. F. Adjadj, E. Belbacha, M. Bouharkat, and A. Kerboub, Crystallographic Study of the Intermediate Compounds SbZn, Sb₃Zn₄ and Sb₂Zn₃, *J. Alloy. Compd.*, 2006, **419**, p 267-270
15. F. Adjadj, E. Belbacha, and M. Bouharkat, Differential Calorimetric Analysis of the Binary System Sb-Zn, *J. Alloy. Compd.*, 2007, **430**, p 85-91
16. F.E. Gallagher, The Alloys of Antimony and Tin, *J. Phys. Chem.*, 1906, **10**, p 93-98
17. K. Iwasé, N. Aoki, and A. Osawa, *Sci. Rep. Tôhoku Univ. Bd*, 1931, **20**, p 353-368
18. A. Stegherr, Doktor-Ingenieurs Genehmigte, Dissertation. Technischen Hochschule, Aachen, 1969
19. H. Ohtani, K. Okuda, and K. Ishida, Thermodynamic Study of Phase Equilibria in the Pb-Sn-Sb System, *J. Phase Equilib.*, 1995, **16**, p 416-429
20. C. Rinco, Order-Disorder Transition in Ternary Chalcopyrite Compounds and Pseudobinary Alloys, *Phys. Rev. B*, 1992, **45**, p 12716
21. A. Tengå, F.J. García-García, and A.S. Mikhaylushkin, Sphalerite-Chalcopyrite Polymorphism in Semimetallic ZnSnSb₂, *Chem. Mater.*, 2005, **17**, p 6080-6085